International Journal of Advanced Biological Science and Engineering, Vol. 2, Issue 1 (2015), Pages 23-34.

ijabse.com

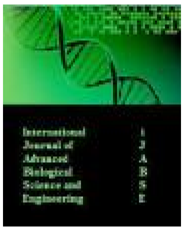

Elliptic Fourier analysis of plastral pigmentation patterns in two populations of Western Hermann's tortoise (Testudo hermanni hermanni)

Pere M. Parés-Casanova*

Department of Animal Production, University of Lleida, Spain.

Abstract

Hermann’s tortoise (Testudo hermanni) is widely distributed in western and southern Europe. As reptiles exhibit strong geographical variation in most morphological, as well as life history traits, gathering data from distant areas is important. Here we used Elliptic Fourier analysis to investigate variation in pigmentation pattern of plastron (ventral shell) of 54 western Hermann's tortoises (T. hermanni hermanni) studied in different private breeders, and belonging to two different Mediterranean populations: Albera (Catalonia, NE Iberian Peninsula, n=14) and Balearic Islands (n=40). Based on this sample, it was shown that plastral pigmentation design does not change between sexes and along animals’ life-history, but differences appeared between geographical populations. These results provide a baseline for further comparisons in variation of plastral pigmentation pattern.

Keywords: image analysis; outline fitting functions; plastral pigmentation pattern; Testudininidae

*Corresponding author at: Department of Animal Production, University of Lleida, Spain.

E–mail address: peremiquelp@prodan.udl.cat

Introduction

Hermann's tortoise (Testudo hermanni GMELIN, 1789) is one of five tortoise species traditionally placed in the genus Testudo, the others being the marginated tortoise (T. marginata), Greek tortoise (T. graeca), Russian tortoise (T. horsfieldii), and Kleinmann's or Egyptian tortoise (T. kleinmanni).

T. hermanni is widely distributed in western and southern Europe, from Catalonia to the Balkans, up to European Turkey (Forlani et al., 2005). Most populations in the western part of the distribution range (e.g. Spain, France and Italy) are severely reduced, whilst the species is still abundant in eastern areas (i.e. the Balkans) (Abdi and Karimi, 2014a; Abdi and Karimi, 2014b). Two subspecies are recognized, T. hermanni hermanni and T. hermanni boettgeri, inhabiting the western (Spain, France, and Italy) and eastern (all other countries) parts of the distribution range, respectively (Gasc et al., 1998). The subspecies T. h. hermanni includes the former subspecies T. h. robertmertensi and has a number of local forms (Abdi et al., 2013a; Abdi et al., 2014a; Abdi et al., 2014b). It has a highly arched shell with an intensive coloration, with its yellow coloration making a strong contrast to the dark patches. The colours wash out somewhat in older animals, but that intense yellow is often maintained. The underside has two connected black bands along the central seam. The coloration of the head ranges from dark green to yellowish, with isolated dark patches (Abdi et al., 2013b; Barati et al., 2014). A particular characteristic is the yellow fleck on the cheek found in most specimens, although not all; T. h. robertmertensi is the name of a morph with very prominent cheek spots. Generally, the forelegs have no black pigmentation pattern on their undersides. The base of the claws is often lightly coloured (Elhamian et al., 2014a; Elhamian et al., 2014b; Faghihi et al., 2014). The tail in males is larger than in females and possesses a spike. Generally, the shell protecting the tail is divided. Pending more definitive data, and with no impact on the subject of our research, we felt justified in employing a conservative species-level taxonomy that retains these two 'classic' subspecies of Testudo, all of which are well-recognized, uncontroversial, monophyletic groups (Javidi et al., 2014a; Javidi et al., 2014b; Karimi et al., 2014f; Karimi et al., 2014g).

As reptiles exhibit strong geographyical variation in most morphological, as well as life history traits, gathering data from isolated areas is important. In this research, we present data from two populations of T. h. hermanni in W Mediterranean, focusing on design of plastral pigmentation pattern (black areas of the ventral shell) (Karimi and Navidbakhsh, 2014a; Karimi and Navidbakhsh, 2014b; Karimi and Navidbakhsh, 2014c).

Varied and efficient methods have been developed to describe and quantify natural objects. The most common ones use superimposition techniques (e.g. Procrustes methods), decomposition into harmonics (Fourier series and functions, wavelets), analysis of spiral functions, and combinations of parameters from elementary geometry (e.g. circularity index, lengthening) (Karimi et al., 2014a; Karimi et al., 2013b).

Since the shape of the plastral pigmentation design is an irregular curved structure, the use of the conventional metrical approach consisting of distances, angles and ratios, was difficult to apply effectively (Karimi et al., 2013a; Karimi et al., 2014l). This shape is too poorly suited for recognition with landmarks and, therefore, the Procrustes-type methods cannot be used. Nevertheless, the morphological variation can be quantified by geometric variables obtained from 2D image analysis of their outlines using an alternative procedure, the elliptic Fourier function (EFF). EFF, developed by (Kuhl and Giardina, 1982), transforms the data from a spatial domain into a frequency domain. They are defined as a parametric formulation in the form: x =

f(t), y = f(t), allowing the separation of the boundary contour into separate x- and y- components. EFF permits the analysis of contours that cannot be simply represented as single-valued functions. Another attractive property of Fourier descriptors is that they not only enable the precise reconstruction of the biological outline, but also permit the re-creation, at any time, of the form from the EFF coefficients, in the absence of the original specimen (Karimi et al., 2014b; Karimi et al., 2014c; Karimi et al., 2014h).

EFF

EFDs have been successfully applied to a number of morphological structures (see (Younker and Ehrlich, 1977), for a review). In recent years a specific FD, the EFF, has been applied to characterize the outline of morphological structures because it allows the analysis of more complex forms than conventional FDs. EFF is ideally suited for characterizing the shape of complex morphologies (Kuhl and Giardina, 1982), but to the authors' knowledge, nothing has been applied to the study of tortoises.

Material and methods

Specimens

In order to analyze plastral pigmentation pattern in western Hermann's tortoise (T. hermanni hermanni), 54 domestic pure animals from authorized private breeders were selected. Their age, according to declaration of keepers, ranged from 6 to 45 months. Forty tortoises were descendants of animals from Balearic Islands and the rest (14) from a continental Iberian area (Albera, NE Iberian Peninsula), both native populations being geographically separated. No differentiation between Balearic Islands was performed, as for some specimens the exact insular origin (Majorca and Minorca) was unknown. Selected animals were sexed, weighed and measured (midline straight carapace length, from the front of the gular scute, to the rear of the carapace). Since in our study we used tortoises randomly collected from different owners, we could not detail life-history variables.

Extraction of the outlines

Ventral image captures were performed with a Nikon (Tokyo, Japan) D70 digital camera (image resolution of 2,240 x 1,488 pixels) equipped with a Nikon AF Nikkor® 28-80 mm telephoto lens. The focal axis of the camera was parallel to the horizontal plane of reference and centred on the plastron (ventral shell). Images included a scale (10 mm x 20 mm). It can be argued that this type of photographic materials can be used with a good reliability as plastrum is very flat, so one does not expect important distortions. The photographs were directly input to computer as GIF files and, subsequently, image noise was manually removed, contour extracted using a graphics software package (Adobe Photoshop version 14.2.1.CC®) (Karimi et al., 2014d; Karimi et al., 2014e; Karimi et al., 2014i), and finally they were transformed to BMP-256 colour files. To avoid redundant information in symmetric structures, only the outline of each left pattern was obtained. Second author (Miralles) was responsible for this "field" part of the research (Karimi et al., 2015; Karimi et al., 2014j; Karimi et al., 2014k; Mohammad Mehdi Elhamian et al., 2014).

Elliptic FDs and multivariate analysis

Image capture was carried out using the SHAPE® software package developed by (Iwata and Ukai, 2002), which identified the outline of the pattern and generated an elliptic Fourier description. Briefly, the procedure was as follows: images were binarized (i.e. transformed into white for the bone outline and black for the background, in pixels) so the outlines of each continuous contour (interface between the black and the white pixels) were automatically obtained and digitalized; the area enclosed in each outline was automatically calculated. Since the coefficients are computed separately for each outline, the outlines need not have the same number of points. An average of 3,290 points was positioned along the outline of each specimen. The coefficients of the elliptic Fourier a_n, b_n, c_n and d_n descriptors, which describe each harmonic, were calculated by the discrete Fourier transformation of the chain-coded contour, the position of the first point being on the standardized outline for all left plastral pigmentation contours. Shape was approximated by the first 20 harmonics (H). Each harmonic corresponded to the four coefficients defining the ellipse on the xy-plane (Razaghi et al., 2014; Shahmohammadi et al., 2014; Shamami et al., 2014). Coefficients were subsequently normalized for size and aligned by the major axis of the ellipse described by first harmonic (H_0) (Kuhl and Giardina, 1982). As SHAPE® adjusted for size and orientation, first harmonic, H_0, does not contain morphological information (CRAMPTON, 1995) and so seventy-six [(4x20)-4] standardized Fourier descriptors were finally considered.

The Fourier coefficients encode the position, orientation, and size of the original data and the starting point on the outline from which digitizing commenced. Adopting these coefficients as a set of transformed variables, they were employed in the analysis. In practice, a number of harmonics less than infinity is used for the summation. A range of harmonics is thus tested and a manageable number is settled on, adequately representing the original curve. In Principal Component Analysis (PCA), we depicted functional relationships. PCA was performed from the covariance matrix. The basic criterion is the maximization of variables' variance, which permitted us to find the optimal rigid axes rotation, axes being the principal components. Geometric interpretation for each principal component was assessed from the reconstructed contours using inverse Fourier transforms. To visualize the variation along a principal component axis, inverse Fourier transforms were calculated for the mean of the Principal Component (PC) scores, with the remaining components set to zero (Iwata and Ukai, 2002). This visualization was helpful to give the morphological meaning of the variation evaluated by each PC (Tehrani et al., 2014a; Tehrani et al., 2014b).

A Kolmogorov-Smirnov test was then used to know the overall equal distribution of male and female samples and a NPMANOVA (Non-Parametric-Multivariate-ANalysis-Of-VAriance, also known as PERMANOVA) test was carried out to know if there were sexual differences, using the Euclidean distances and nine separately as independent variables (log transformed), and coefficients as dependent ones. As regression has a number limit for dependent variables, only six harmonics (H_1 to H_6) were considered. A Multivariate-ANalysis-Of-VAriance (MANOVA) tested the multivariate regression significances using the Wilks' lambda test statistic as the ratio of determinants. Finally, a new NPMANOVA was carried out in order to study geographical differences in shape. For both NPMANOVA, nine harmonics (H_1 to H_9) were considered, as it will be seen that additional harmonics do not increase the accuracy of the reconstruction (FATURECHI et al., 2014; Karimi and Navidbakhsh, 2014d).

The statistical treatment was performed with the PAST® package (Hammer et al., 2001). The significance level was established at 5%.

Results

Differences between sexes

Preliminary analyses revealed no significant different distribution between males and females (D=0.290, p=0.189) and, as no differences appeared between sexes (p=0.689), data from both populations were pooled for further analyses.

Regression on body weight and length

Neither of the regressions of form on log body weight (505.5g±297.1, range 100-1,260g) and length (121.7mm±26.8, range 66-171.7mm) were significant (R^2=0.05, *Wilk's* λ=0.204 and R^2=0.04, *Wilk's* λ=0.185, p<<<0.0001, respectively), so an isometric change of plastral pigmentation pattern can be supposed along life and/or corporal condition of animals.

Quantitative analysis of the elliptic Fourier descriptors

The first 9 Principal Components explained 85.2% of the total variance observed (Table 1). Summary statistics of the elliptic Fourier descriptors of these 9 harmonics for the size-normalized plastral pigmentation outlines studied are listed in Table 2. Their representations are given in Figure 1.

Table 1. Results of the Principal Component Analysis for first 9 Principal Components. These first Principal Components explained 85.2% of the total variance observed. Almost no change at all was observed for any reconstruction using more harmonics.

Principal Component (PC)	Eigenvalue	Proportion of variance (%)	Cumulative variance (%)
PC1	0.00741	40.68	40.68
PC2	0.00248	13.50	54.26
PC3	0.00147	8.06	62.33
PC4	0.00112	6.15	68.48
PC5	0.00088	4.80	73.29
PC6	0.00072	3.94	77.23
PC7	0.00054	2.94	80.18
PC8	0.00050	2.72	82.91
PC9	0.00042	2.32	85.23

Figure 1. Elliptic Fourier analysis of the left plastral pigmentation outlines of the 54 western Hermann's tortoise (T. hermanni hermanni) studied. Representations of the harmonics corresponding to the first 9 Principal Components (PC).

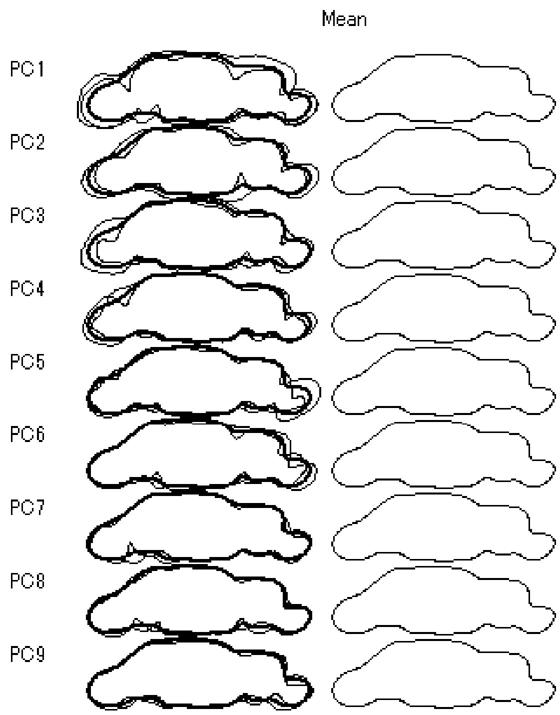

Table 2. Summary statistics (mean and standard deviation, S.D.) for size-normalized left plastral pigmentation outlines of the elliptic Fourier descriptors (a_n, b_n, c_n and d_n) of the first 9 harmonics (H_1 to H_9) (H_0 excluded).

	a_n		b_n		c_n		d_n	
Harmonics	Mean	S.D.	Mean	S.D.	Mean	S.D.	Mean	S.D.
1	1.00000		0.00000		0.00000		0.32776	
2	0.00226	0.03494	0.06898	0.06092	-0.11217	0.02859	-0.01055	0.02357
3	0.04823	0.02434	-0.01883	0.02547	0.01487	0.01694	0.00307	0.02272
4	-0.00280	0.01592	0.02201	0.02745	-0.03585	0.02264	0.01049	0.01729
5	0.03892	0.01376	-0.01112	0.02167	0.00032	0.02317	0.02583	0.01972
6	-0.00343	0.01755	-0.00482	0.01635	0.00393	0.01598	-0.01192	0.01603
7	0.01555	0.01470	-0.01087	0.01443	0.01270	0.01927	0.01138	0.01720
8	0.00614	0.01382	0.00208	0.01570	0.00849	0.01565	-0.00281	0.02043
9	0.01837	0.01330	-0.00037	0.01060	0.01026	0.01889	0.01277	0.01437

Differences between populations

Statistical differences appeared between populations ($p=0.0048$). Plastral designs for both populations appear in Figure 2.

Figure 2. Plastral right designs for both populations (Albera and Balearic Islands). On bottom part, gular scutes on left, anal plaques on right for each picture.

Albera Balearic Islands

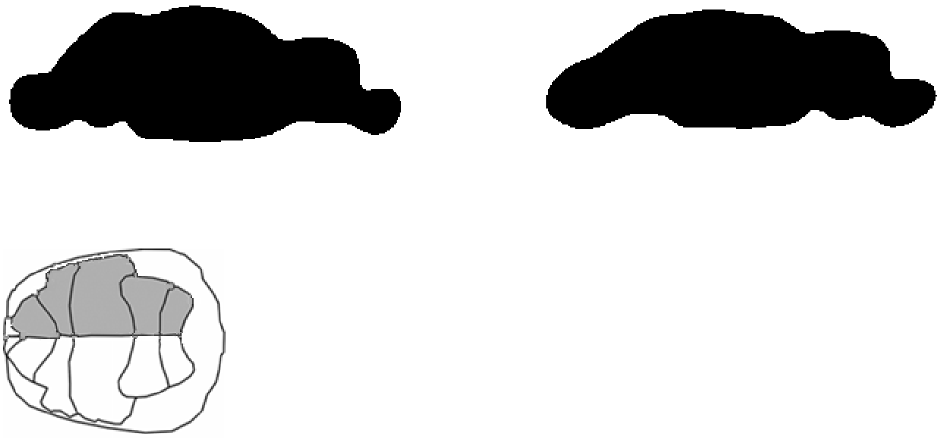

Discussion

From data in this research, plastral pigmentation pattern can be deduced as a good phenotypic trait, with similarity between sexes and not related to life-history of animals, but with differences between some geographical populations. For this research, we studied two populations, and it would be interesting to have information for more populations, both insular and continental. Evidently, we could not exclude that they may be a product of random differentiation, and no molecular data are available, so authors do not intend to draw any taxonomical conclusion. However, what seems absolutely clear is that the study of plastral pigmentation pattern with Elliptic methods, although time-consuming and mathematically complex, can provide a baseline for further comparisons between populations to examine small geographical variation in Testudo hermanni, as it can distinguish subtle variations in the plastral pigmentation shape which are difficult to describe with mere descriptive qualitative methods.

The outlines employed in the present study turned out to be an example of apparently very complex data that are very well-suited for a particular analysis. Because EFA relies on the identification of the major axis of the best-fitting ellipse to achieve the requisite standardizations, the fact that the plastral pigmentation outline is not circular for the outlines in the current data set makes the use of such standardizations very tenable. In conclusion, the results here are considered encouraging and suggest the need for the initiation of further research to discover more accurate geometrical descriptors of the plastral pigmentation pattern in Testudo hermanni.

Sources of funding

None to declare.

Conflicts of interest statement

The authors declare that they are no conflicts of interests.

Acknowledgements
Authors are absolutely grateful to owners who kindly allowed the study of their animals.

References

Abdi, M., Karimi, A., 2014a. A computational electrical analogy model to evaluate the effect of internal carotid artery stenosis on circle of willis efferent arteries pressure. Journal of Biomaterials and Tissue Engineering 4, 749-754.

Abdi, M., Karimi, A., 2014b. Stress distribution analysis in healthy and pathologic knee joint: A finite element study. International Journal of Advanced Biological Science and Engineering 1.

Abdi, M., Karimi, A., Navidbakhsh, M., Hassani, K., Faghihi, S., 2013a. Modeling of cerebral aneurysm using equivalent electrical circuit (Lumped Model). Perfusion 29, 142-152.

Abdi, M., Karimi, A., Navidbakhsh, M., Pirzad Jahromi, G., Hassani, K., 2014a. A lumped parameter mathematical model to analyze the effects of tachycardia and bradycardia on the cardiovascular system. International Journal of Numerical Modelling: Electronic Networks, Devices and Fields. DOI: 10.1002/jnm.2010.

Abdi, M., Karimi, A., Navidbakhsh, M., Rahmati, M., Hassani, K., 2014b. MODELING OF CORONARY ARTERY BALLOON-ANGIOPLASTY USING EQUIVALENT ELECTRICAL CIRCUIT. Biomedical Engineering: Applications, Basis and Communications 26, 1450039-1450049.

Abdi, M., Karimi, A., Navidbakhsh, M., Rahmati, M., Hassani, K., Razmkon, A., 2013b. Modeling the Circle of Willis Using Electrical Analogy Method under both Normal and Pathological Circumstances. Journal of Biomedical Physics and Engineering 3.

Barati, E., Halabian, M., Karimi, A., Navidbakhsh, M., 2014. Numerical evaluation of stenosis location effects on hemodynamics and shear stress through curved artery. Journal of Biomaterials and Tissue Engineering 4, 358-366.

CRAMPTON, J. S., 1995. Elliptic Fourier shape analysis of fossil bivalves: some practical considerations. Lethaia 28, 179-186.

Elhamian, M. M., Karami, H., Alizadeh, M., Shokrieh, M. M., Karimi, A., 2014a. Model for analyzing the mechanical behavior of articular cartilage under creep indentation test. Journal of Applied Physics 116, 184702184711.

Elhamian, M. M., Alizadeh, M., Shokrieh, M. M., Karimi, A., Madani, P., 2014b. An innovative randomly oriented laminated composite model for articular cartilage tissue. Journal of Biomaterials and Tissue Engineering 4, 645-650.

Faghihi, S., Gheysour, M., Karimi, A., Salarian, R., 2014. Fabrication and mechanical characterization of graphene oxide-reinforced poly (acrylic acid)/gelatin composite hydrogels. Journal of Applied Physics 115, 083513-083520.

FATURECHI, R., KARIMI, A., HASHEMI, A., YOUSEFI, H., NAVIDBAKHSH, M., 2014. Influence of Poly (acrylic acid) on the Mechanical Properties of Composite Hydrogels. Advances in Polymer Technology. DOI 10.1002/adv.21487

Forlani, A., Crestanello, B., Mantovani, S., Livoreil, B., Zane, L., Bertorelle, G., Congiu, L., 2005. Identification and characterization of microsatellite markers in Hermann's tortoise (Testudo hermanni, Testudinidae). Molecular Ecology Notes 5, 228-230.

Gasc, J.-P., Cabela, A., Crnobrnja-Isailovic, D., Dolmen, K., Grossenbacher, K., Haffner, P., Lescure, J., Martens, H., Martinez-Rica, J. P., Maurin, H., 1998. Atlas of amphibians and reptiles in Europe. Copeia.

Hammer, Ø., Harper, D., Ryan, P., 2001. PAST-Palaeontological statistics. www. uv. es/~ pardomv/pe/2001_1/past/pastprog/past. pdf, acessado em 25, 2009.

Iwata, H., Ukai, Y., 2002. SHAPE: a computer program package for quantitative evaluation of biological shapes based on elliptic Fourier descriptors. Journal of Heredity 93, 384-385.

Javidi, M., Heydari, M., Karimi, A., Haghpanahi, M., Navidbakhsh, M., Razmkon, A., 2014a. Evaluation of the Effects of Injection Velocity and Different Gel Concentrations on Nanoparticles in Hyperthermia Therapy. Journal of Biomedical Physics and Engineering 4.

Javidi, M., Heydari, M., Attar, M., Haghpanahi, M., Karimi, A., Navidbakhsh, M., Amanpour, S., 2014b. Cylindrical agar gel with fluid flow subjected to an alternating magnetic field during hyperthermia. International Journal of Hyperthermia, 1-7. DOI: 10.3109/02656736.2014.988661.

Karimi, A., Navidbakhsh, M., 2014a. An experimental study on the mechanical properties of rat brain tissue using different stress–strain definitions. Journal of Materials Science: Materials in Medicine, 1-8. DOI 10.1007/s10856-014-5198-0.

Karimi, A., Navidbakhsh, M., 2014b. A comparative study on the uniaxial mechanical properties of the umbilical vein and umbilical artery using different stress–strain definitions. Australasian Physical & Engineering Sciences in Medicine, 1-10.

Karimi, A., Navidbakhsh, M., 2014c. Measurement of the nonlinear mechanical properties of a poly (vinyl alcohol) sponge under longitudinal and circumferential loading. Journal of Applied Polymer Science 131. DOI: 10.1002/APP.40257.

Karimi, A., Navidbakhsh, M., 2014d. Material properties in unconfined compression of gelatin hydrogel for skin tissue engineering applications. Biomedical Engineering/Biomedizinische Technik 59, 479-486.

Karimi, A., Navidbakhsh, M., Haghi, A. M., 2014a. An experimental study on the structural and mechanical properties of polyvinyl alcohol sponge using different stress–strain definitions. Advances in Polymer Technology 33. DOI 10.1002/adv.21441.

Karimi, A., Navidbakhsh, M., Razaghi, R., 2014b. Dynamic simulation and finite element analysis of the human mandible injury protected by polyvinyl alcohol sponge. Materials Science and Engineering: C 42, 608-614.

Karimi, A., Navidbakhsh, M., Razaghi, R., 2014c. An experimental-finite element analysis on the kinetic energy absorption capacity of polyvinyl alcohol sponge. Materials Science and Engineering: C 39, 253-258.

Karimi, A., Navidbakhsh, M., Razaghi, R., 2014d. A finite element study of balloon expandable stent for plaque and arterial wall vulnerability assessment. Journal of Applied Physics 116, 044701-044710.

Karimi, A., Navidbakhsh, M., Razaghi, R., 2014e. Plaque and arterial vulnerability investigation in a three-layer atherosclerotic human coronary artery using computational fluid-structure interaction method. Journal of Applied Physics 116, 064701-064710.

Karimi, A., Navidbakhsh, M., Shojaei, A., 2015. A combination of histological analyses and uniaxial tensile tests to determine the material coefficients of the healthy and atherosclerotic human coronary arteries. Tissue and Cell, doi:http://dx.doi.org/10.1016/j.tice.2015.01.004.

Karimi, A., Navidbakhsh, M., Haghi, A. M., Faghihi, S., 2013a. Measurement of the uniaxial mechanical properties of rat brains infected by Plasmodium berghei ANKA. Proc IMechE Part H: J Engineering in Medicine, 227, 609-614.

Karimi, A., Navidbakhsh, M., Haghi, A. M., Faghihi, S., 2013b. An innovative shape equation to quantify the morphological characteristics of parasitized red blood cells by Plasmodium falciparum and Plasmodium vivax. Proc IMechE Part H: J Engineering in Medicine, 227, 428-437.

Karimi, A., Abdi, M., Navidbakhsh, M., Haghi, A. M., 2014f. An image method to characterize the morphological properties of parasitized red blood cells by Plasmodium falciparum-A review study. International Journal of Advanced Biological Science and Engineering 1.

Karimi, A., Haghighatnama, M., Navidbakhsh, M., Haghi, A. M., 2014g. Measurement of the axial and circumferential mechanical properties of rat skin tissue at different anatomical locations. Biomedical Engineering/Biomedizinische Technik. DOI: 10.1515/bmt-2014-0084.

Karimi, A., Navidbakhsh, M., Haghighatnama, M., Haghi, A. M., 2014h. Determination of the axial and circumferential mechanical properties of the skin tissue using experimental testing and constitutive modeling. Computer Methods in Biomechanics and Biomedical Engineering, 1-7. DOI: 10.1080/10255842.2014.961441.

Karimi, A., Navidbakhsh, M., Razaghi, R., Haghpanahi, M., 2014i. A computational fluid-structure interaction model for plaque vulnerability assessment in atherosclerotic human coronary arteries. Journal of Applied Physics 115, 144702-144711.

Karimi, A., Navidbakhsh, M., Rezaee, T., Hassani, K., 2014j. Measurement of the circumferential mechanical properties of the umbilical vein: experimental and numerical analyses. Computer Methods in Biomechanics and Biomedical Engineering, 1-9. DOI: 10.1080/10255842.2014.910513.

Karimi, A., Navidbakhsh, M., Yamada, H., Razaghi, R., 2014k. A nonlinear finite element simulation of balloon expandable stent for assessment of plaque vulnerability inside a stenotic artery. Medical & Biological Engineering & Computing, 52, 589-599.

Karimi, A., Navidbakhsh, M., Haghi, A. M., Faghihi, S., 2014l. A morphology-based method for the diagnosis of red blood cells parasitized by Plasmodium malariae and Plasmodium ovale. Scandinavian Journal of Infectious Diseases 46, 368-375.

Kuhl, F. P., Giardina, C. R., 1982. Elliptic Fourier features of a closed contour. Computer graphics and image processing 18, 236-258.

Mohammad Mehdi Elhamian, S., Alizadeh, M., Mehrdad Shokrieh, M., Karimi, A., Pejman Madani, S., 2014. Transversely isotropic micromechanics model to determine effect of collagen fibre angle in mechanical properties of articular cartilage. Materials Technology: Advanced Performance Materials 29, 377-383.

Ravandi, A. K., Karimi, A., Navidbakhsh, M., 2014. Numerical analysis for nonlocal nonlinear vibration of a double layer graphene sheet integrated with ZnO piezoelectric layers. Journal of Vibration and Control, 1077546314561036.

Razaghi, R., Karimi, A., Navidbakhsh, M., Jarrahi, A., 2014. Determination of the vulnerable plaque in a stenotic human coronary artery-finite element modeling. Perfusion, DOI: 0267659114557720.

Shahmohammadi, M., Shirazi, H. A., Karimi, A., Navidbakhsh, M., 2014. Finite element simulation of an artificial intervertebral disc using fiber reinforced laminated composite model. Tissue and Cell, 46, 299-303.

Shamami, D. Z., Karimi, A., Beigzadeh, B., Haghpanahi, M., Navidbakhsh, M., 2014. A 3D finite element study for stress analysis in bone tissue around single implants with different materials and various bone qualities. Journal of Biomaterials and Tissue Engineering 4, 632-637.

Tehrani, P., Rahmani, S., Karimi, A., Alizadeh, M., Navidbakhsh, M., 2014a. Modeling of Balloon Part of a New Cardiac Assist Device Known as AVICENA. Journal of Biomaterials and Tissue Engineering 4, 772-777.

Tehrani, P., Rahmani, S., Karimi, A., Alizadeh, M., Navidbakhsh, M., 2014b. A novel cardiac assist device (AVICENA): A numerical study to compute the generated power. Perfusion, 0267659114547943.

Younker, J. L., Ehrlich, R., 1977. Fourier biometrics: harmonic amplitudes as multivariate shape descriptors. Systematic Biology 26, 336-342.